Biochemical and Biophysical Research Communications xxx (2017) 1–8

Contents lists available at ScienceDirect

Biochemical and Biophysical Research Communications

journal homepage: www.elsevier.com/locate/ybbrc

Multiscale approach to the activation and phosphotransfer mechanism of CpxA histidine kinase reveals a tight coupling between conformational and chemical steps

Franco Marsico [a, b, 1], Osvaldo Burastero [a, b, 1], Lucas A. Defelipe [a, b], Elias Daniel Lopez [a, b], Mehrnoosh Arrar [c], Adrián G. Turjanski [a, b, *], Marcelo A. Marti [a, b, *]

[a] Departamento de Química Biológica, Facultad de Ciencias Exactas y Naturales, Universidad de Buenos Aires, Intendente Güiraldes 2620, Ciudad Autónoma de Buenos Aires, Argentina
[b] IQUIBICEN-UBA/CONICET, Intendente Güiraldes 2620, Ciudad Autónoma de Buenos Aires, Argentina
[c] Instituto de Química-Física de los Materiales, Medio Ambiente y Energía, CONICET-Facultad de Ciencias Exactas y Naturales, Universidad de Buenos Aires, Buenos Aires, Argentina

ARTICLE INFO

Article history:
Received 15 June 2017
Received in revised form
23 August 2017
Accepted 8 September 2017
Available online xxx

Keywords:
Coarse grain
QM/MM
Histidine kinase
CpxA
Two component system

ABSTRACT

Sensor histidine kinases (SHKs) are an integral component of the molecular machinery that permits bacteria to adapt to widely changing environmental conditions. CpxA, an extensively studied SHK, is a multidomain homodimeric protein with each subunit consisting of a periplasmic sensor domain, a transmembrane domain, a signal-transducing HAMP domain, a dimerization and histidine phospho-acceptor sub-domain (DHp) and a catalytic and ATP-binding subdomain (CA). The key activation event involves the rearrangement of the HAMP-DHp helical core and translation of the CA towards the acceptor histidine, which presumably results in an autokinase-competent complex.

In the present work we integrate coarse-grained, all-atom, and hybrid QM-MM computer simulations to probe the large-scale conformational reorganization that takes place from the inactive to the autokinase-competent state (conformational step), and evaluate its relation to the autokinase reaction itself (chemical step). Our results highlight a tight coupling between conformational and chemical steps, underscoring the advantage of CA walking along the DHp core, to favor a reactive tautomeric state of the phospho-acceptor histidine. The results not only represent an example of multiscale modelling, but also show how protein dynamics can promote catalysis.

1. Introduction

Ubiquitous two-component systems are the macromolecular machinery underlying the survival of bacteria in changing environments [1–3]. Upon detection of a specific environmental stimulus, the first component, a sensor histidine kinase (SHK) initiates a phosphorelay to the second component, its cognate receptor, which in turn modulates gene expression. SHKs are generally homodimers that are themselves structurally modular and minimally comprise two domains, the *N*-terminal sensor domain, and the *C*-terminal histidine kinase domain. Often a variable number of signal-transducing or transmembrane domains are found in between, and all of the contiguous domains are connected by a central coiled-coil alpha-helical axis. The histidine kinase domain itself is made up of two sub-domains; the dimerization and histidine phospho-acceptor sub-domain (DHp), which is part of the alpha-helical axis, and the catalytic and ATP-binding subdomain (CA), which is connected to the axis via flexible linkers [4].

To initiate the phospho-relay, a signal received at the sensor domain must be transmitted to the distant histidine kinase domain, causing the rearrangement of the CA subdomains into an autokinase-competent conformation, a process that is still not completely understood [5–8]. The tuning of the structural rearrangements in the histidine kinase domain is even more complex when considering that the same histidine kinase domain must also adopt phosphotransferase- and phosphatase-competent conformations in order to couple properly with its cognate receptor

* Corresponding authors.
E-mail addresses: adrian@qi.fcen.uba.ar (A.G. Turjanski), marti.marcelo@gmail.com (M.A. Marti).
[1] Both authors contributed equally to this work.

http://dx.doi.org/10.1016/j.bbrc.2017.09.039
0006-291X/

[9–11].

CpxA is a widely studied SHK that works as an environmental stress sensor in *E. coli*, and has been found to be activated by the presence of misfolded proteins or at high pH [12]. CpxA consists of (from *N*- to *C*-terminus) a periplasmic sensor domain, a transmembrane domain, a signal-transducing HAMP domain, followed by its histidine kinase domain, which belongs to the pfam HisKA family (Fig. 1) [13]. Crystallographic structures of the cytoplasmic region of CpxA in an inactive state depict an overall symmetric conformation in which the ATP-loaded CA is far (ca. 20 A) from the phosphoacceptor His248. A constitutively active variant of CpxA has also been crystallized, interestingly, in a tentative autokinase-competent conformation and as an asymmetric dimer, in which one CA-bound ATP gamma phosphate lies within reactive distance (ca. 4 A) of the phosphoacceptor (Fig. 1B) [14]. A doubly phosphorylated state has been also suggested to exist, accessible through sequential autophosphorylation events, as there is no structural evidence yet for a symmetrical doubly-active conformation [15].

A comparison of the inactive and autokinase-competent conformations highlights the necessary conformational changes implicated in CpxA activation; that is, a significant translation of one CA with respect to the DHp, as well as intrinsic changes in the HAMP and DHp (Fig. 1B). How these changes in the HAMP-DHp core induce the repositioning of one of the two ATP-loaded CA subdomains is still unclear, yet essential for understanding the transmission of information through the protein matrix and allosteric processes in general. Moreover, although the proposed active conformations depict several expected features of an autokinase-competent ternary complex, further evidence of its catalytic capacity and the underlying details of the autophosphorylation reaction itself are still lacking. Finally, it is important to note that for CpxA, and SHKs in general, there is little information that unifies the conformational rearrangements and chemical steps involved in the transition from the inactive to the autophosphorylated histidine kinase states, a process that seems to be the rate-limiting step in the overall signal transmission in bacterial two-component systems.

To address this gap, we have used a multi-scale approach, combining coarse-grained (CG), all-atom (AA), and hybrid quantum-mechanical/molecular-mechanical (QM/MM) simulations to evaluate the conformational transition of CpxA between inactive and autokinase-competent states, and the implications of this conformational transition on the autophosphorylation reaction itself. Our results show that the overall activation of CpxA can be divided into the initial activation of the HAMP-DHp domains, a process that triggers the subsequent reorientation of the ATP-loaded CA domain, and that these conformational changes closely modulate the pKa of the phospho-accepting His residue, which we show to be key in the autophosphorylation reaction mechanism [5].

2. Computational methods

2.1. Starting structures

Autokinase-competent (active) and inactive conformations were taken from the PDB database (crystal structures 4BIV and 4BIX respectively [14]. The active structure corresponds to the cytosolic portion of CpxA that includes HAMP, DHp and CA domains. Unfortunately in the inactive structure only the Dhp and CA domains are resolved. To model the missing HAMP domain, the MODELLER software was used [16], using the structure of chimeric Af1503 HAMP - EnvZ DHp homodimer (2LFR) as template [17].

2.2. All-atom molecular dynamics simulation parameters

All-atom molecular dynamics simulations of both conformational states of CpxA cytosolic domain were performed using the PMEMD [18] module of the AMBER14 [19] package with the FF14SB force field [20] in explicit TIP3P [21] solvent with 0,2 M of NaCl concentration. All simulations were performed at 300 K and constant pressure using the berendsen barostat. Parameters for ATP were taken from the literature [22]. For each case, production dynamics of 100 ns with a time step of 2 fs were performed.

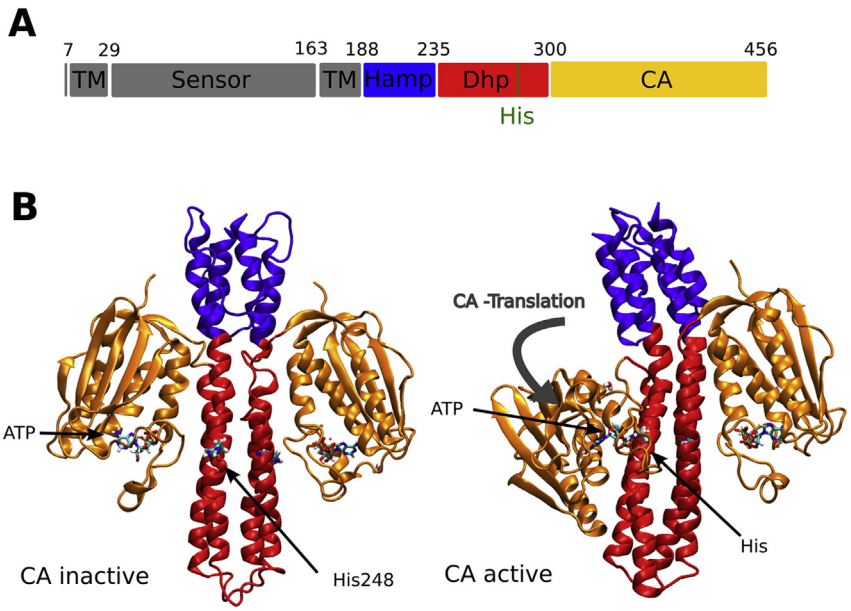

Fig. 1. A) Domain structure of full length CpxA. B) Cytosolic domains of CpxA in two different conformations. Inactive (Left, 4BIX) and autokinase-competent (Right, 4BIW) structures of cytosolic CpxA highlighting their key differences. The unsolved HAMP domain of the inactive structure was modeled as described in methods.

Please cite this article in press as: F. Marsico, et al., Multiscale approach to the activation and phosphotransfer mechanism of CpxA histidine kinase reveals a tight coupling between conformational and chemical steps, Biochemical and Biophysical Research Communications (2017), http://dx.doi.org/10.1016/j.bbrc.2017.09.039

2.3. Coarse grained model

CG simulations were performed using a in-house modified version of the PMEMD module of AMBER11, where the CG force field developed by Voth et al. [23] was implemented. In order to further reduce the computational cost of the molecular simulations Generalized Born model of implicit solvent with a salt concentration of 0,2 M (NaCl) was used. CG representation allowed us to use a 4 fs time step [24]. Initial structures were converted to the CG representation, minimized, and slowly thermalized to the desired temperature using the Langevin thermostat. Coarse grain ATP parametrization was performed as described in our previous work [27] and parameters are available under request. All simulations were performed at constant pressure using Berendsen barostat. In both cases, test equilibrium simulations were performed at 100, 125, 150 and 160 K. Results at 150 K were more accurate considering RMSD and essential dynamics (ED) [25] analysis in comparison with the results observed in all-atom simulations (Table S1 and S2). Essential dynamics (ED) analysis (of the C_α atoms) and projection of the MD trajectories onto selected essential modes were also performed on the combined CG trajectories in order to gain insight and obtain a quantitative parameter for the structural transition. The backmapping approach was used in order to obtain an atomistic representation of transition structures [24]. The DHp-CA interdomain contact energy was estimated using a simple residue-residue contact model [26].

2.4. Steered molecular dynamics

To study the transition between the two conformational states of CpxA we used steered Molecular Dynamics (sMD) with the CG model, using RMSD as a reaction coordinate, as implemented in our previous work [27]. We tested two different approaches. In the first one (one-step activation) the pulling force was applied to the HAMP-DHp domains as well as to the ATP-loaded CA; in the second (step-wise activation) first the HAMP-DHp domains were steered and the transition of the ATP-loaded CA was carried out in a separate process. For the one-step approach a pulling velocity of 11.8 A/ns was used, whereas for the stepwise activation a pulling velocity of 12.09 A/ns and 0.058 A/ns was used was used for the first and second steps, respectively, with a force constant of 30 kcal/molA^2 for all cases.

2.5. Constant pH molecular dynamics

With the aim of investigating the protonation state of the phospho-acceptor histidine 248 along the conformational change, the active, inactive and 4 transition conformations obtained from backmapped coarse grain structure were used as starting points to run all-atom constant pH molecular dynamics (CpHMD). In this method, developed by Mongan et al. [28], and previously used in our group [29], the titratable residue changes its protonation and tautomeric state according to its electrostatic environment. CpHMD of 2 ns at pH 7 and 300 K with the backbone harmonically restrained (with a force constant of 2 kcal/molA^2) were carried out for the six different structures.Subsequently the fraction of the simulation that histidine spent in each protonation state was extracted.

2.6. Reaction free energies using hybrid QM(DFT-GGA)/MM simulations

To compute the free energy profile (FEP) for the autophosphorylation reaction we used sMD combined with a QM/MM scheme based on a GPU implementation of a Density Functional Theory method with the Generalized Gradient Approximation (DFT GGA), developed and tested by our group [30]. The QM/MM implementation works with the AMBER molecular dynamics package and force field and is freely available [31]. As a starting point for each sMD trajectory, 16 equilibrated snapshots were taken at 1-ps intervals from a QM/MM simulation of the reactant state. The starting structures for QM/MM simulations were derived from the corresponding all-atom classical MD simulations, after cooling to 10 K. Thus, each QM/MM systems was slowly heated to 300 K independently to allow proper equilibration. We considered four different QM/MM systems, three of which correspond to variants of the phosphoryl transfer in the protein matrix, and one in which we consider the same reaction in water. For the main scheme in the protein matrix, the QM region comprised the side chain of the autophosphorylable histidine 248 and the conserved glutamate 249, the triphosphate arm of ATP (from the C5′ atom to the γ-phosphate), a Mg^{2+} ion, two waters and the side chain of asparagine 360 implicated in Mg coordination. We also built the same system but with a protonated ATP, and mutating the conserved glutamate to leucine. Finally, a capped histidine and ATP were used to study the reaction in water. Covalent boundaries between QM and MM system were treated with the Link atom method, as implemented in AMBER. For all QM atoms, the calculations were performed with the PBE [32] functional using the DZVP basis, except for magnesium for which we used a 6-31G basis.

The chosen reaction coordinate was in all cases a combination of the interatomic distances related with the phosphoryl transfer reaction:

$$\lambda(\mathrm{r}) = \mathrm{d}(P^{\gamma} - N^{\varepsilon}) - \mathrm{d}\left(P^{\gamma} - O^{\beta}\right) \tag{3}$$

The pulling speed was $\frac{0.23}{ps}$ and the arbitrary constant was 300 kcal/mol/A^2. The Jarzynski estimator was used to compute the FEP (more details in SI) [33].

3. Results

To study the conformational transition from the inactive to the autokinase-competent (or active) state, we first analyzed the stability and dynamical properties of each state. For the inactive state PDB id 4BIX was used as the initial structure, and the missing HAMP domain was modeled using PDB id 2LFR as a template. For the active state PDB id 4BIV was used as the initial structure, as the gamma-phosphate of AMPPNP is within reactive distance of phosphoacceptor His248. Both states were modeled with ATP-Mg2+ bound to both CA domains. A total of 1 microsecond of coarse-grained (CG) simulations were carried out for each state, both of which remained close to their initial conformations, reaching stability at RMSD values of 4 and 5.5 Å in the active and inactive conformations respectively. The dynamics observed in the CG simulations were also cross-checked against all-atom simulations, confirming by RMSIP analysis that the CG model accurately reproduced the protein's overall plasticity (Table S2).

By concatenating the inactive and active state trajectories, and aligning along the central alpha-helical axis, the transition essential modes (EM) were computed from the covariance matrix [34]. The first EM (Fig. 2A) describes a counter-clockwise rotation of the HAMP helices concurrent with a clockwise rotation of the *C*-terminal end of the DHp helices and a small reorientation of the CA domain. The second EM comprises a slight bending of the alpha-helical axis and the large translation of the CA domain, thus altering the CA-DHp interface. Qualitatively similar modes were obtained by considering the EM of the HAMP-DHp domains and the CA domains independently.

After characterizing the inactive and active conformational

Please cite this article in press as: F. Marsico, et al., Multiscale approach to the activation and phosphotransfer mechanism of CpxA histidine kinase reveals a tight coupling between conformational and chemical steps, Biochemical and Biophysical Research Communications (2017), http://dx.doi.org/10.1016/j.bbrc.2017.09.039

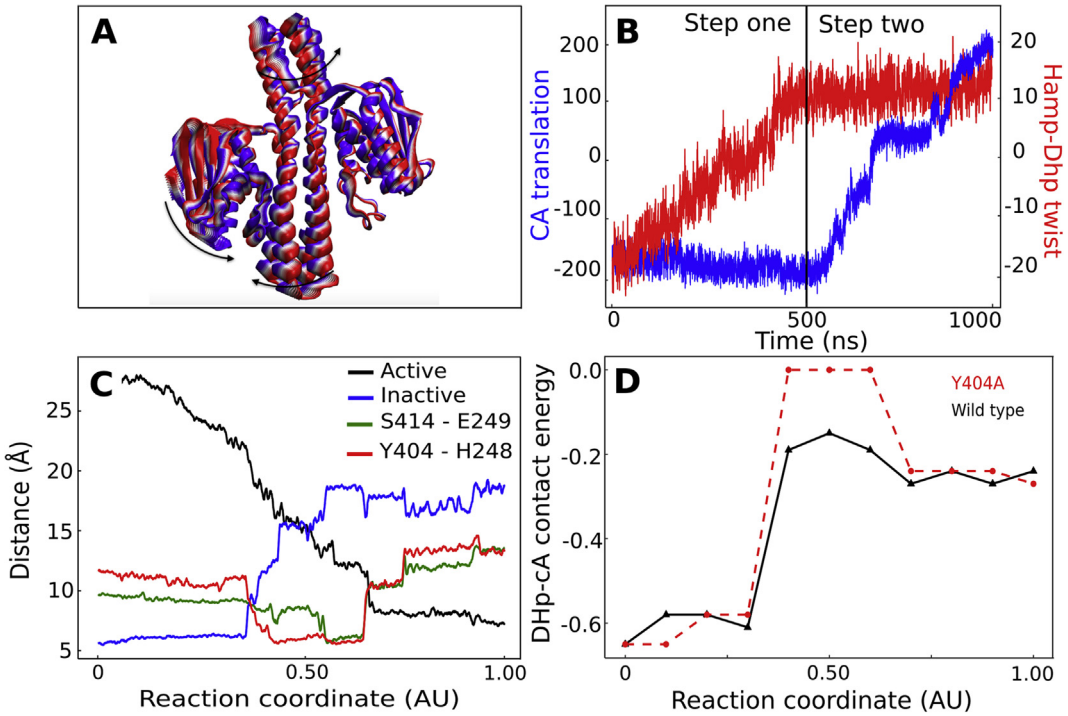

Fig. 2. A) Decomposition of CpxA structural transition in Single domain motions B) Projection of CG CpxA sMD trajectories on the transition essential modes. The reference values for each conformation are, for the CA translation, −200 (inactive) and 200 (active) and for the Hamp-DHp twist −20 (inactive) and 20 (active). Step one and two correspond to the activation of the HAMP-DHp and CA, respectively. C) Evolution of selected DHp-CA contacts during the two step transition. Active (black) and Inactive (blue) corresponds to the average distance of the residues that interact in each conformation D) DHp-CA contact energy in RT units. The reaction coordinate was normalized such that 0 and 1 correspond to the inactive and active structures respectively, and is expressed in arbitrary units (AU). (For interpretation of the references to colour in this figure legend, the reader is referred to the web version of this article.)

states, we used sMD to drive the conformational transition in both directions, using the RMSD to the target structure as the reaction coordinate. Applying a CG model in sMD simulation imply some advantages: first, the selected CG force field does not require an explicit nor continuum water model (long range interactions are modeled as effective potentials) and second, each CG particle represents about 5–15 atoms. Consequently, there is a significant reduction in system size and complexity of the underlying energy landscape that allows to sample conformational transitions in an efficient way, in terms of both computational cost and structural detail.

We considered two scenarios for the conformational transition: a concerted approach in which the force was applied to the HAMP-DHp as well as to the “mobile” CA domain; and, alternatively, a step-wise approach in which first the force was applied exclusively to the HAMP-Dhp domains, and subsequently to the mobile CA domain. We observed that the concerted path was largely dominated by the translation of the CA domain, such that the RMSD from the target structure could be substantially reduced without allowing the full conformational transition of the HAMP-Dhp domains. Indeed, by projecting the RMSD-driven sMD trajectories onto the independent domain transition modes, we observed that the HAMP-DHp domains only achieved approximately one third of the full transition (Figure S1). On the contrary, in the step-wise approach the HAMP-Dhp domains are fully activated according to both RMSD and the independent domain transition mode. Furthermore, activation of the HAMP-DHp alone induces the onset of the CA domain reorientation, underscoring the connection between the two processes. In the second segment of the step-wise approach, the conformational transition is completed, as shown in Fig. 2B. A cross-RMSD analysis of the sMD trajectories in the forward and reverse directions show that the path is microscopically reversible and thus allows observation of key events driving the transition (Figure S2).

Detailed analysis of the transitions, shows that activation of the HAMP-DHp domains results in two key events. The unwinding of the *C*-terminal portion of the Dhp α-2 helix, (residues 299 to 305) which is converted into a gamma-turn, and the loss of key CA-Dhp interactions (Fig. 2C). As a consequence of these two events, the CA domain is released from its inactive state, and then starts to move. It is important to note that the CA domain is not completely released, rather it starts to walk “counter-clockwise” along the DHp surface. As shown in Fig. 2C, key transient contacts between the CA and DHp domain are maintained as the CA domain approaches the phosphoacceptor. In particular, Tyr404 plays a critical role in this activation “walk”, forming a transient hydrogen bond with His248. To gain detailed insight into the changing interactions between the CA and DHp during activation, intermediate structures from CG sMD trajectories were back-mapped into an all-atom resolution and simulated for 20 ns, from which the interdomain contact energy was calculated. These results highlight the importance of Tyr404 in the conformational transition, since its replacement with alanine results in a loss of the favorable interdomain contact energy during the process (Fig. 2D). Fig. 2C may suggest that S414 plays a similar role to Y404. However, mutation analysis of S414 showed that is has no significant effect on the DHp-CA interaction during the transition (data not shown).

One of the main consequences of the observed walking of the CA during the conformational transitions is a substantial change in the His 248 phosphoacceptor environment; though initially solvent-exposed, His248 is quickly buried and establishes specific hydrogen bonds with CA domain residues until the gamma

Please cite this article in press as: F. Marsico, et al., Multiscale approach to the activation and phosphotransfer mechanism of CpxA histidine kinase reveals a tight coupling between conformational and chemical steps, Biochemical and Biophysical Research Communications (2017), http://dx.doi.org/10.1016/j.bbrc.2017.09.039

phosphate of the bound ATP approaches. We wondered how this effect would influence the tautomeric equilibrium of the phosphoacceptor, and consequently, the phosphoryltransfer reaction. It is important to note, that the autophosphophosphorylation reaction requires that His248 be in its neutral imidazole state (Fig. 3), specifically with the epsilon nitrogen deprotonated in order to attack the gamma phosphate. In the protonated imidazolium state (HIP) the reactive nitrogen must first transfer a proton before autophosphorylation can occur. His tautomer/protonation state equilibria is subtle (N_δ and N_ε microscopic pKa are both close to 6–7) and are actively regulated in many proteins. Therefore, we analyzed histidine tautomeric preference during the activation of CpxA, as the CA approaches His248, using constant pH MD simulations with initial structures taken from the coarse-grained sMD conformational transition, after first back-mapping into an all-atom resolution.

The results, presented in Fig. 3C show that in the inactive state His 248 is predominantly in the HIP state. Protonation of the N_δ is maintained by a strong hydrogen bond with the highly conserved Glu249, a result that is consistent with site-directed mutagenesis studies in other HKs including NtrB [35] and CdrS [36], explaining its essential role for kinase activity. When the CA starts to specifically interact with His248, it displaces the equilibrium towards the HID tautomeric state, due to formation of a hydrogen bond with Tyr404 (Fig. 3A). Though this preference for the HID tautomeric state is maintained during the structural transition, it changes abruptly in the simulations of the "proposed" autokinase-competent or active state, as protonated His (HIP) is again the preferred state, once negatively charged ATP is in close proximity (Fig. 3C). Indeed, any attempts to simulate the active conformation with His248 in any of the neutral imidazole states (HID or HIE) resulted in a less stable conformation as compared to simulations of the HIP state (data not shown). Taken together, the coarse-grained conformational transition and all-atom constant pH simulations suggest two possible mechanistic scenarios for the autophosphorylation of CpxA: either the autophosphorylation occurs in a concerted fashion with the conformational inactive-to-active transition, or, upon activation His248 must first donate its N_e proton before the phophoryl-transfer reaction can occur.

To address these two scenarios, and to study in detail the phosphoryl-transfer reaction in CpxA, we determined the free energy profiles associated with the different proposed mechanisms using QM/MM-based steered molecular dynamics at the DFT(PBE/DZVP) level [32]. We first considered the stable active conformation from the classical MD simulations, with His248 in HIP state, and evaluated the possibility of ATP accepting the proton. No other possible proton acceptor was observed in five independent classical 200 ns MD trajectories with His248 in the HIP state. We found that proton transfer to ATP was plausible, requiring about 4 kcal/mol (Figure S3). Nevertheless, the free energy profiles for the subsequent phosphoryl transfer reaction (Fig. 4A) shows that the nucleophilic attack of the gamma phosphate of protonated ATP comprises a very large barrier (>25 kcal/mol) similar to that of the uncatalyzed reaction in water and yields an unstable product state. On the other hand, when the neutral HID tautomer reacts with ATP in its completely ionized form, the barrier is only 16 kcal/mol, reflecting how the protein environment stabilizes the transition state, as compared to the reaction in solution. Therefore, these results strongly suggest that the autophosphorylation reaction is tightly coupled to the conformational transition itself, and that the stable active conformation observed in the crystal structure is possibly a trapped conformation, likely due to the use of a non-hydrolyzable ATP analog.

Detailed analysis of the structural and electronic parameters

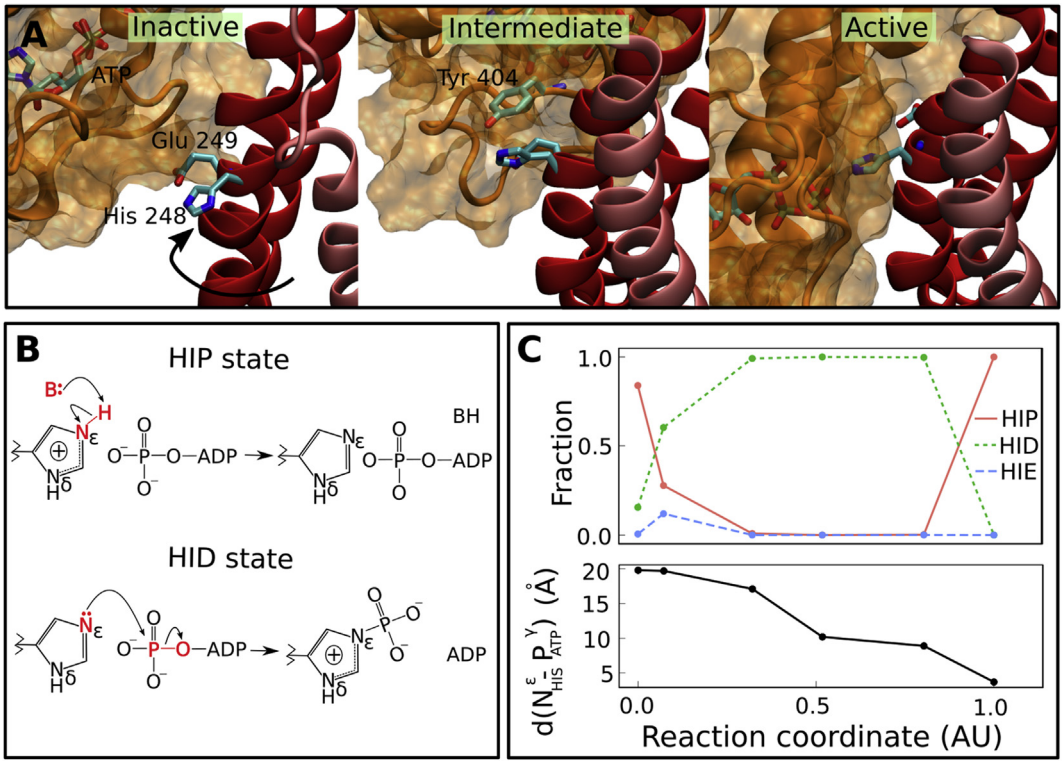

Fig. 3. A) close up of inactive (left), intermediate (middle) and active (right) DHp structures highlighting the environment of phospho-acceptor His248 B) His tautomers in relation to its phospho acceptor capacity C) His tautomer preference at pH 7 and His-ATP distance as function of the normalized reaction coordinate, with 0 and 1 corresponding to the inactive and active states, respectively.

Please cite this article in press as: F. Marsico, et al., Multiscale approach to the activation and phosphotransfer mechanism of CpxA histidine kinase reveals a tight coupling between conformational and chemical steps, Biochemical and Biophysical Research Communications (2017), http://dx.doi.org/10.1016/j.bbrc.2017.09.039

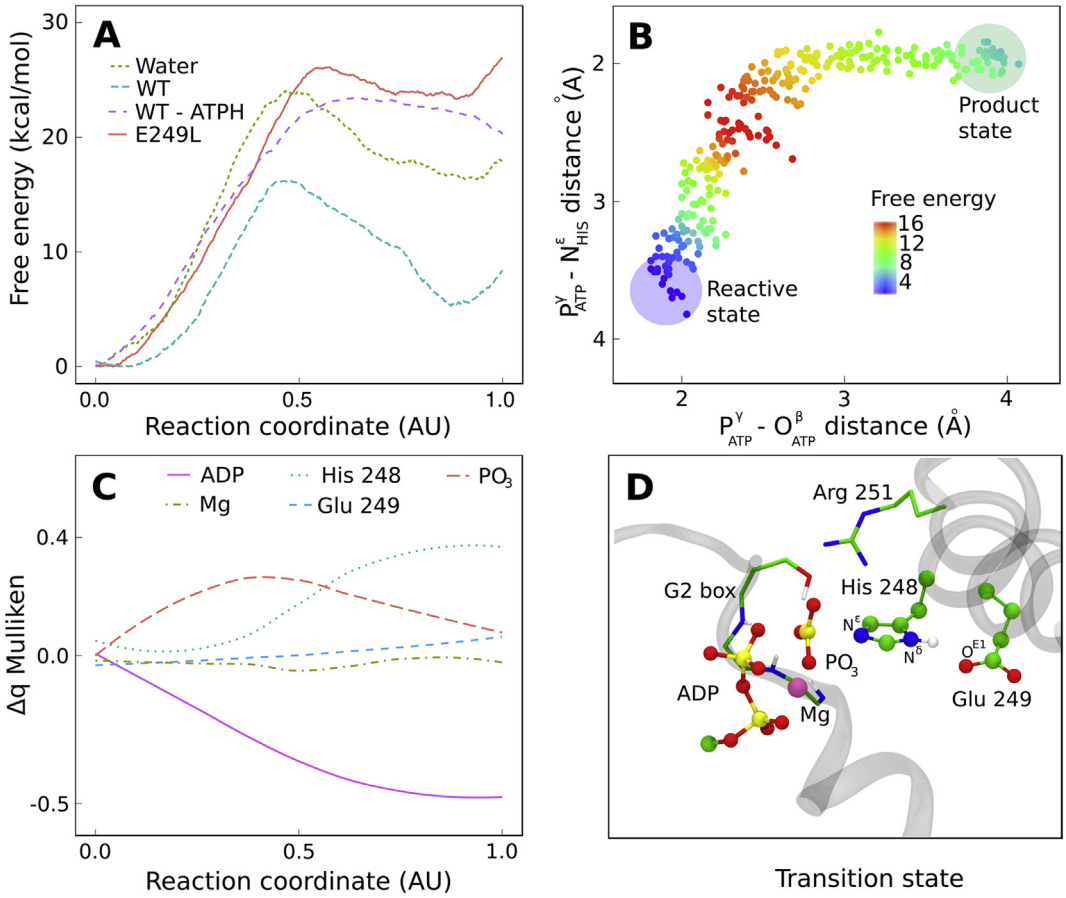

Fig. 4. A) Free energy profile for three variants of the phosphoryl-transfer reaction in CpxA and in water. B) Corresponding MOFJ plot of the Protein reaction using bond forming and bond breaking distances from one representative sMD. C) Mulliken charge change along the reaction coordinate. The selected moieties were the side chains from His248 and Glu249, the magnesium ion, ADP and the phosphoryl group. In all cases the reaction coordinate was normalized such that 0 and 1 correspond to the inactive and active states, respectively. D) An atomistic representation of the transition state.

along the reaction coordinate (Fig. 4B and C and SI) shows that the reaction displays a concerted mechanism with a very symmetric S_N2 pentavalent transition state (TS), with the trigonal phosphate equally distant from the histidine nucleophile and ADP. The TS is directly stabilized by three hydrogen bonds from the conserved G2 box motif and electrostatic interactions with conserved Arg251. Moreover, the reaction mutating Glu249 to a leucine (E249L), therefore maintaining a similar volume but removing the negative charge, results again in a high energy barrier (of approximately 25 kcal/mol) and an unstable product state. The FEP of the E249L mutant correlates well with experimental findings, showing that mutations of this glutamate in other HKs such as NtrB [35] and CdrS [36] led to kinase dead phenotypes and an acidic residue at this position is highly conserved (90% of HK sequences), and when absent in sequence, another spatially equivalent acid appears to take its position [14].

As shown in Fig. 4A and D, the glutamate stabilizes the TS indirectly and the phosphohistidine directly by hydrogen bonding with the N_δ; contributing to the nucleophilic character of the N_ε. This is in good agreement with performed phosphohistidine vacuum geometry optimizations (S. Table 3 and S Table 4), in which the *N*-P bond is shorter when the phosphohistidine δ nitrogen is not protonated. (H1E versus H1P and H2E versus H2P). Also, it was previously suggested that the Glu249 could act as a general base to fully capture the histidine δ hydrogen [37]. A distance analysis between the histidine H_δ and glutamic oxygen displays, that in fact, not a complete, but a partial proton transfer occurs (Figure S4). Thus the H_δ is increasingly shared as the reaction progresses. Overall, the participation of all these residues suggest a conserved reaction mechanism among histidine kinases. The More O'Ferrall–Jencks (MOFJ) plot (Fig. 4B) reveals that the reaction has some associative character too. The HIS-phosphate bond (y - axis) must be slightly formed before the ADP-phosphate bond (x - axis) breaks. In other words, the nucleophilic attack is prior to the departure of the leaving group. Last, we performed a qualitative analysis of the evolution of the Mulliken charges along the reaction coordinate. A considerable charge change from the histidine which starts neutral and ends positively charged gaining 0.5 of mulliken charge units was found. The ADP moiety finishes negatively charged and the transferred phosphoryl group is only modestly charged in the transition state (0.5 in the normalized reaction coordinate).

4. Discussion

SHKs are hallmark examples of allosteric signal transduction proteins, and as such have been intensively studied from a structural dynamic point of view [38–41]. The current view sustains that upon signal detection by the sensor domain, a structural change is transmitted to the HAMP-DHp helical core, which results in displacement of the CA and results in an autokinase-competent state [42,43]. Despite detailed knowledge of the inactive and active end states, little is known about the dynamics of the transition, the coupling between subdomains, and more important how, and if, the conformational step is related to the chemical step

Please cite this article in press as: F. Marsico, et al., Multiscale approach to the activation and phosphotransfer mechanism of CpxA histidine kinase reveals a tight coupling between conformational and chemical steps, Biochemical and Biophysical Research Communications (2017), http://dx.doi.org/10.1016/j.bbrc.2017.09.039

and the underlying phosphoryltransfer mechanism. Studying the complete SHK activation process, explicitly considering the conformation and chemical steps, using molecular simulation tools represents a considerable challenge, and requires the ability to synergistically combine QM-based models to study chemical reactions with simplified models to probe the conformational step. We undertook this challenge combining a CG model to characterize the structural transition, which is back-mapped to an AA representation to obtain further detail, leading finally to a QM/MM analysis of the chemical step, thus representing a paradigmatic example of multiscale modelling.

Our results imply that the CA domain does not diffuse freely from the inactive to the autokinase-competent conformation, i.e there is no release of the CA by the DHp during activation. Instead, the CA "walks" along the DHp, and although the CA is connected to the DHp by a flexible linker loop which becomes unstructured upon activation, the CA is not necessarily completely released. On the contrary, the activation of the HAMP-DHp alone prompts the reorientation of the CA domain. In this sense we identified contacts between the CA and DHp domains that are maintained and make the transition energetically favorable. The walking has important consequences since it allows precise thermodynamic guiding of the CA towards the active conformation, and also results in a fine tuning of the tautomeric state of His248, allowing it to become phosphorylated, and thus ultimately controlling the chemical step. Our data interestingly show that conformational and chemical steps must be tightly coupled and occur almost concertedly, since once the active state conformation is reached, His248 becomes protonated and blocked. This coupling could be interpreted as a direct contribution of protein dynamics to catalysis, a topic of intense debate in the recent years [44–46].

Another more subtle but nonetheless relevant result of the observed CA walking, concerns the relationship between HAMP-DHp supercoiling and cis versus trans phosphorylation. The walking naturally biases the CA towards the His284 that is encountered first in a counter-clockwise CA translation, which follows the relative rotation of the HAMP helices. This directionality of HKs nicely fits with the observation made by Laub and Marina [15,47] showing that cis vs trans autophosphorylation is linked to the topology of the DHp domain, which can be determined (but not predicted) by the sequence of the DHp loops at the bottom of the helix bundle [48]. If the biased directionality observed here for CpxA is conserved among the HisKA family, then the CA domains are always guided counter-clockwise, effectively phosphorylating in cis or trans, depending on the topology of the DHp itself.

Acknowledgments

This work was supported by grants PICT 2015-2276, PICTO GSK 2012-0057 and PIP 11220130100469CO awarded to AGT and MAM. The authors would like to thank Centro de Cómputos de Alto Rendimiento (CeCAR), FCEN-UBA and TUPAC-CSC-CONICET for granting use of computational resources which allowed us to perform the experiments included in this work. OB is a CONICET doctoral fellow. LAD and MA are CONICET postdoctoral fellows. AGT and MAM are members of the CONICET.

We also thank Dr. Adrián Roitberg, Quantum Theory Project, University of Florida, for granting use of computational resources and for helpful discussions.

Appendix A. Supplementary data

Supplementary data related to this article can be found at http://dx.doi.org/10.1016/j.bbrc.2017.09.039.

References

[1] D. Albanesi, M.C. Mansilla, D. De Mendoza, et al., The membrane fluidity sensor DesK of Bacillus subtilis controls the signal decay of its cognate response regulator, J. Bacteriol. 186 (2004) 2655–2663, 186.
[2] D. y, T.J. Silhavy, P.N. Danese, W.B. Snyder, et al., The Cpx two-component signal transduction pathway of Escherichia coli regulates transcription of the gene specifying the stress-inducible periplasmic protease, DegP, Genes Dev. 15 (1995) 387–398, 9.
[3] J. Rinaldi, M. Arrar, G. Sycz, et al., Structural insights into the HWE histidine kinase family: the Brucella blue light-activated histidine kinase domain, J. Biol. Mol. 24 (2016) 4247–4259.
[4] R. Dutta, L. Qin, M. Inouye, Microreview histidine kinases: diversity of domain organization 34 (1999) 633–640.
[5] H.U. Ferris, S. Dunin-Horkawicz, N. Hornig, M. Hulko, J. Martin, J.E. Schultz, K. Zeth, A.N. Lupas, M. Coles, Mechanism of regulation of receptor histidine kinases, Structure 20 (2012) 56–66.
[6] C.M., L.A.N., H.U. Ferris, M.D. Hartmann, Crystallographic snapshot of the Escherichia coli EnvZ histidine kinase in an active conformation, J. Struct. Biol. 186 (2014) 1–4.
[7] R.P. Diensthuber, M. Bommer, T. Gleichmann, A. Möglich, Full- length structure of a sensor histidine kinase pinpoints coaxial coiled coils as signal transducers and modulators, Structure 106 (2013) 1127–1136.
[8] D. Albanesi, M. Marti, F. Trajtenberg, et al., Structural plasticity and catalysis regulation of a thermosensor histidine kinase, PNAS 106 (2014) 6185–16190.
[9] P.M. Wolanin, P.A. Thomason, J.B. Stock, Protein family review Histidine protein kinases: key signal transducers outside the animal kingdom, (2002) 1–8.
[10] A.E. Mechaly, S. Soto Diaz, N. Sassoon, et al., Structural coupling between autokinase and phosphotransferase reactions in a bacterial histidine kinase, Structure 24 (2017) 4247–4259.
[11] F. Trajtenberg, J.A. Imelio, M.R. Machado, N. Larrieux, M.A. Marti, G. Obal, A.E. Mechaly, A. Buschiazzo, Regulation of signaling directionality revealed by 3D snapshots of a kinase: regulator complex in action, Elife 5 (2016) e21422.
[12] S. Nakayama, H. Watanabe, Involvement of cpxA, a sensor of a two-component regulatory system, in the pH-dependent regulation of expression of Shigella sonnei virF gene, J. Bacteriol. 177 (1995) 5062–5069, 177.
[13] W.A. C.J. y Hendrickson, J. Cheung, W.A. Hendrickson, Sensor domains of two-component regulatory systems, Curr. Opin. Microbiol. 13.2 (2010) 116–123, 13.
[14] A.E. Mechaly, N. Sassoon, J.M. Betton, P.M. Alzari, Segmental helical motions and dynamical asymmetry modulate histidine kinase autophosphorylation, PLoS Biol. 12 (2014).
[15] P. M.-R.L.M.A. y Casino, P. Casino, L. Miguel-Romero, A. Marina, P. Casino, L. Miguel-Romero, Visualizing autophosphorylation in histidine kinases, Nat. Commun. 5 (2014) 3258.
[16] A. Šali, T.L. Blundell, Comparative protein modelling by satisfaction of spatial restraints, J. Mol. Biol. 234 (1993) 779–815.
[17] Ferris HU1, S. Dunin-Horkawicz, N. Hornig, et al., Mechanism of regulation of receptor histidine kinases, Structure 20 (2012) 56–66.
[18] R. Salomon-Ferrer, A.W. Götz, D. Poole, S. Le Grand, R.C. Walker, Routine microsecond molecular dynamics simulations with AMBER on GPUs. 2. Explicit solvent particle mesh Ewald, J. Chem. Theory Comput. 9 (2013) 3878–3888.
[19] D.A. Case, R.M. Betz, W. Botello-Smith, et al., AMBER 2016, Univ. California, San Fr, 2016.
[20] J.A. Maier, C. Martinez, K. Kasavajhala, L. Wickstrom, K.E. Hauser, C. Simmerling, ff14SB: improving the accuracy of protein side chain and backbone parameters from ff99SB, J. Chem. Theory Comput. 11 (2015) 3696–3713.
[21] W.L. Jorgensen, J. Chandrasekhar, J.D. Madura, R.W. Impey, M.L. Klein, Comparison of simple potential functions for simulating liquid water, J. Chem. Phys. 79 (1983) 926–935.
[22] K.L. Meagher, L.T. Redman, H.A. Carlson, Development of polyphosphate parameters for use with the AMBER force field, J. Comput. Chem. 24 (2003) 1016–1025.
[23] R.D. Hills Jr., L. Lu, G. Voth, Multiscale coarse-graining of the protein energy landscape, PLoS Comput. Biol. (2010) 1–12.
[24] L.E.L.M.A.M. y Luciana Capece, L.E. Lombardi, M.A. Mart'\i, L. Capece, CG2AA: backmapping protein coarse-grained structures, Bioinforma 32 (2015) 1235–1237, 32.
[25] A. Amadei, A. Linssen, H.J.C. Berendsen, Essential dynamics of proteins, Proteins Struct. Funct. Bioinforma. 17 (1993) 412–425.
[26] S. Miyazawa, R.L. Jernigan, Self-consistent estimation of inter-residue protein contact energies based on an equilibrium mixture approximation of residues, Proteins Struct. Funct. Bioinforma. 34 (1999) 49–68.
[27] C.L. Ramírez, A. Petruk, M. Bringas, D.A. Estrin, A.E. Roitberg, M.A. Marti, L. Capece, Coarse-grained simulations of heme proteins: validation and study of large conformational transitions, J. Chem. Theory Comput. 12 (2016) 3390–3397.
[28] J. Mongan, D.A. Case, J.A. McCAMMON, Constant pH molecular dynamics in generalized born implicit solvent, J. Comput. Chem. 25 (2004) 2038–2048.
[29] L.A. Defelipe, E. Lanzarotti, D. Gauto, M.A. Marti, A.G. Turjanski, Protein topology determines cysteine oxidation fate: the case of sulfenyl amide

formation among protein families, PLoS Comput. Biol. 11 (2015) e1004051.
[30] M.A. Nitsche, M. Ferreria, E.E. Mocskos, M.C. Gonzalez Lebrero, GPU accelerated implementation of density functional theory for hybrid QM/MM simulations, J. Chem. Theory Comput. 10 (2014) 959–967.
[31] LIO Project, (n.d.). https://github.com/MALBECC/lio.
[32] J.P. Perdew, K. Burke, M. Ernzerhof, Generalized gradient approximation made simple, Phys. Rev. Lett. 77 (1996) 3865.
[33] C.L. Ram'\irez, M.A. Mart'\i, A.E. Roitberg, Chapter six-steered molecular dynamics methods applied to enzyme mechanism and energetics, Methods Enzymol. 578 (2016) 123–143.
[34] M.A. Marti, D.A. Estrin, A.E. Roitberg, Molecular basis for the pH dependent structural transition of Nitrophorin 4, J. Phys. Chem. B 113 (2009) 2135–2142.
[35] M.R. Atkinson, A.J. Ninfa, Mutational analysis of the bacterial signal-transducing protein kinase/phosphatase nitrogen regulator II (NRII or NtrB), J. Bacteriol. 175 (1993) 7016–7023.
[36] J.W. Willett, J.R. Kirby, Genetic and biochemical dissection of a HisKA domain identifies residues required exclusively for kinase and phosphatase activities, PLoS Genet. 8 (2012) e1003084.
[37] A. Marina, C. Mott, A. Auyzenberg, W.A. Hendrickson, C.D. Waldburger, Structural and mutational analysis of the PhoQ histidine kinase catalytic domain insight into the reaction mechanism, J. Biol. Chem. 276 (2001) 41182–41190.
[38] A. Möglich, R.A. Ayers, K. Moffat, Design and signaling mechanism of light-regulated histidine kinases, J. Mol. Biol. 385 (2009) 1433–1444.
[39] H.U. Ferris, S. Dunin-Horkawicz, L.G. Mondéjar, et al., The mechanisms of HAMP-mediated signaling in transmembrane receptors.,, Structure 19 (2011) 378–385.
[40] C.L.-L., J.A. Appleman, V. Stewart, Probing conservation of HAMP linker structure and signal transduction mechanism through analysis of hybrid sensor kinases, J. Bacteriol. 185 (2003) 4872–4882.
[41] J.S. Parkinson, Signaling mechanisms of HAMP domains in chemoreceptors and sensor kinases, Annu. Rev. Microbiol. 64 (2010) 101–122.
[42] M. Hulko, F. Berndt, M. Gruber, et al., The HAMP domain structure implies helix rotation in transmembrane signaling, Cell 126 (2006) 929–940.
[43] A.D. Gutu, K.J. Wayne, L.T. Sham, M.E. Winkler, Kinetic characterization of the WalRKSpn (VicRK) two-component system of Streptococcus pneumoniae: dependence of WalKSpn (VicK) phosphatase activity on its PAS domain, J. Bacteriol. 192 (2010) 2346–2358.
[44] A. Warshel, R.P. Bora, Perspective: defining and quantifying the role of dynamics in enzyme catalysis, J. Chem. Phys. 144 (2016) 180901.
[45] J.P. Klinman, A. Kohen, Hydrogen tunneling links protein dynamics to enzyme catalysis, Annu. Rev. Biochem. 82 (2013) 471–496.
[46] K.A. Henzler-Wildman, M. Lei, V. Thai, S.J. Kerns, M. Karplus, D. Kern, A hierarchy of timescales in protein dynamics is linked to enzyme catalysis, Nature 450 (2007) 913–916.
[47] E.J. Capra, M.T. Laub, Evolution of two-component signal transduction systems, Annu. Rev. Microbiol. 66 (2012) 325–347.
[48] O. Ashenberg, A.E. Keating, M.T. Laub, Helix bundle loops determine whether histidine kinases autophosphorylate in cis or in trans, J. Mol. Biol. 425 (2013) 1198–1209.

Please cite this article in press as: F. Marsico, et al., Multiscale approach to the activation and phosphotransfer mechanism of CpxA histidine kinase reveals a tight coupling between conformational and chemical steps, Biochemical and Biophysical Research Communications (2017), http://dx.doi.org/10.1016/j.bbrc.2017.09.039